Mononuclear and Trinuclear Dy^{III} SMMs with Schiff-base Ligands Modified by Nitro- Group: First Triangular Complex with N-N Pathway

Li-Wei Cheng, [a] Chi-Lung Zhang,[a] Jun-Yu Wei,[a] Po-Heng Lin*[a]

[a] Department of Chemistry, National Chung Hsing University, 250 Kuo Kuang Rd., Taichung 402, Taiwan. Email: poheng@dragon.nchu.edu.tw; Tel: + 886-4-22840411, ext. 724

Supporting Information

Experimental

X-ray Crystallographic Studies

Single crystals of complexes **1**-**3** suitable for X-ray diffraction measurements were mounted on the Bruker D8 VENTURE and the unit cell was determined using Bruker SMART APEX 3 software suite to employ graphite-monochromated Mo-Kα radiation (λ = 0.71073 Å), and intensity data were collected with ω scans. The data collection and reduction were performed with the *CrysAlisPro* software, and the absorptions were corrected by the *SCALE3 ABSPACK* multiscan method. The space-group determination was based on a check of the Laue symmetry and systematic absences, and it was confirmed using the structure solution. The structure was solved and refined with the *Olex2 1.2-ac21 package*. Anisotropic thermal parameters were used for all non-H atoms, and fixed isotropic parameters were used for H atoms.

Magnetic Measurement

Direct current (dc) magnetic susceptibility measurements were performed on a Quantum Design MPMS7 magnetometer equipped with a 7.0 T magnet, operating in the range of 2.0–300.0 K. Alternating current (ac) susceptibility measurements were carried out on Quantum Design PPMS-9 magnetometer equipped with a 9.0 T magnet and operating in the range of 1.8–300 K. Ac frequencies ranging from 100 to 10000 Hz and temperatures ranging from 1.8 to 30 K. Diamagnetic corrections were estimated from Pascal's constant and subtracted from the experimental susceptibility data to determine.

Table S1 Crystallographic data of complexes **1**, **2** and **3**.

Complex	**1**	**2**	**3**	**4**
Formula	$C_{23}H_{32}DyN_9O_{14}$	$C_{32}H_{36}DyN_9O_{17}$	$C_{69}H_{81}Dy_3N_{24}O_{33}$	$C_{69}H_{81}Gd_3N_{24}O_{33}$
Formula weight	821.07	981.20	2262.07	2246.32
Temp (K)	150(2) K	150(2) K	150(2) K	150(2) K
Crystal system	monoclinic	monoclinic	cubic	cubic
Space group	$P12_1/n1$	P12/c1	Pa-3	Pa-3
a (Å)	14.480(4)	10.6293(5)	28.873(3)	28.897(4)
b (Å)	15.745(5)	13.9322(7)	28.873(3)	28.897(4)
c (Å)	15.510(5)	13.7379(7)	28.873(3)	28.897(4)
α (deg)	90	90	90	90
β (deg)	115.989(14)	112.566(2)	90	90
γ (deg)	90	90	90	90
V(Å^3)	3178.5(17)	1878.68(16)	24070(8)	24130(10)
Z	4	2	8	8
D_{calc}(g/cm^3)	1.716	1.735	1.248	1.237
μ(Mo Kα) (mm^{-1})	2.431	2.078	1.914	1.700
F(000)	1644.0	986.0	9000.0	8952.0
N_{ref}, N_{par}	6482, 431	8203, 283	7887, 394	8235, 394
$R1[I > 2\sigma(I)]$	0.0295	0.0285	0.0714	0.0613
w$R2$ $[I > 2\sigma(I)]$	0.0796	0.0752	0.1857	0.1531
S	1.128	1.034	1.044	1.184

Table S2 Selected angle and bond lengths (Å) for complex **1**.

∠O1-Dy1-O11	124.77(9)	∠O2-Dy1-O8	146.10(10)
∠O1-Dy1-O12	79.42(9)	∠O2-Dy1-O7	78.40(9)
∠O1-Dy1-O9	72.14(9)	∠O2-Dy1-N3	70.66(9)
∠O1-Dy1-O8	69.97(9)	∠O12-Dy1-O11	51.94(9)
∠O1-Dy1-N3	63.37(9)	∠O12-Dy1-O9	73.81(10)
∠O6-Dy1-O1	84.89(9)	∠O12-Dy1-O8	122.82(10)
∠O6-Dy1-O11	150.28(9)	∠O12-Dy1-N3	72.88(10)
∠O6-Dy1-O12	150.85(10)	∠O9-Dy1-O11	70.55(9)
∠O6-Dy1-O9	124.20(10)	∠O9-Dy1-O8	51.54(10)
∠O6-Dy1-O8	73.01(10)	∠O9-Dy1-N3	128.01(10)
∠O6-Dy1-O7	83.25(10)	∠O8-Dy1-O11	112.61(10)
∠O6-Dy1-N3	78.14(10)	∠O8-Dy1-N3	126.52(9)
∠O11-Dy1-N3	114.70(10)	∠O7-Dy1-O1	143.97(9)
∠O2-Dy1-O1	134.01(9)	∠O7-Dy1-O11	71.26(9)
∠O2-Dy1-O6	84.61(10)	∠O7-Dy1-O12	123.15(9)
∠O2-Dy1-O11	75.70(10)	∠O7-Dy1-O9	86.89(10)
∠O2-Dy1-O12	88.81(10)	∠O7-Dy1-O8	74.04(9)
∠O2-Dy1-O9	145.99(9)	∠O7-Dy1-N3	145.05(9)
Dy1-O1	2.415(3)	Dy1-O9	2.470(3)
Dy1-O6	2.283(3)	Dy1-O8	2.504(3)
Dy1-O11	2.519(3)	Dy1-O7	2.367(2)
Dy1-O2	2.245(2)	Dy1-N3	2.569(3)
Dy1-O12	2.435(3)		

Table S3 Selected angle and bond lengths (Å) for complex **2**.

∠N3-Dy01-N3	97.34(7)	∠O2-Dy01-O2A	118.58(7)
∠O1-Dy01-N3	146.91(5)	∠O2-Dy01-O6	77.99(6)
∠O1-Dy01-N3	63.90(5)	∠O2-Dy01-O6A	156.18(5)
∠O1-Dy01-N3	63.90(5)	∠O2A-Dy01-O6	156.18(5)
∠O1-Dy01-N3	146.91(5)	∠O2A-Dy01-O6A	77.99(6)
∠O1-Dy01-O1	144.93(7)	∠O6-Dy01-N3A	135.26(5)
∠O2-Dy01-N3	72.08(5)	∠O6-Dy01-N3	101.75(6)
∠O2-Dy01-N3	68.48(5)	∠O6A-Dy01-N3	135.26(5)
∠O2-Dy01-N3	68.48(5)	∠O6A-Dy01-N3A	101.75(6)
∠O2-Dy01-N3	72.08(5)	∠O6-Dy01-O1A	78.67(5)
∠O2-Dy01-O1	119.36(5)	∠O6-Dy01-O1	77.26(5)
∠O2-Dy01-O1	119.36(5)	∠O6A-Dy01-O1	78.67(5)
∠O2-Dy01-O1A	79.48(5)	∠O6A-Dy01-O1A	77.26(5)
∠O2A-Dy01-O1	79.48(5)	∠O6-Dy01-O6	92.42(9)
Dy01-O1	2.5260(16)	Dy01-O6	2.2980(14)
Dy01-O1A	2.5259(16)	Dy01-O6A	2.2980(14)
Dy01-O2	2.3806(13)	Dy01-N3	2.3132(15)
Dy01-O2A	2.3806(13)	Dy01-N3A	2.3132(15)

Table S4 Selected angle and bond lengths (Å) for complex **3**.

∠N2-Dy01-N3	79.8(2)	∠O1-Dy01-O11	74.5(2)
∠N5-Dy01-N2	125.7(2)	∠O1-Dy01-O5	137.1(2)
∠N5-Dy01-N3	62.8(2)	∠O1-Dy01-O9	130.4(2)
∠O10-Dy01-N2	146.0(3)	∠O5-Dy01-N2	64.5(2)
∠O10-Dy01-N3	89.9(3)	∠O5-Dy01-N3	85.1(2)
∠O10-Dy01-N5	74.9(2)	∠O5-Dy01-N5	74.0(2)
∠O11-Dy01-N2	74.7(2)	∠O5-Dy01-O10	147.2(2)
∠O11-Dy01-N3	152.6(2)	∠O5-Dy01-O11	92.5(2)
∠O11-Dy01-N5	142.3(2)	∠O9-Dy01-N2	132.4(2)
∠O11-Dy01-O10	106.0(3)	∠O9-Dy01-N3	131.8(2)
∠O1-Dy01-N2	72.6(2)	∠O9-Dy01-N5	69.0(2)
∠O1-Dy01-N3	88.7(2)	∠O9-Dy01-O10	77.7(3)
∠O1-Dy01-N5	138.1(2)	∠O9-Dy01-O11	74.4(2)
∠O1-Dy01-O10	75.0(2)	∠O9-Dy01-O5	81.7(2)
Dy01-N2	2.531(7)	Dy01-O10	2.378(7)
Dy01-N3	2.546(8)	Dy01-O11	2.375(7)
Dy01-N5	2.527(7)	Dy01-O5	2.304(6)
Dy01-O1	2.236(6)	Dy01-O9	2.295(6)

Table S5 Summary of *SHAPE*[1] analysis for complexes **1**, **2** and **3**.

Vertices	Code	Label	Shape	Symmetry
9	1	EP-9	Enneagon	D_{9h}
	2	OPY-9	Octagonal pyramid	C_{8v}
	3	HBPY-9	Heptagonal bipyramid	D_{7h}
	4	JTC-9	Triangular cupola (J3) = trivacant cuboctahedron	C_{3v}
	5	JCCU-9	Capped cube (Elongated square pyramid, J8)	C_{4v}
	6	CCU-9	Capped cube	C_{4v}
	7	JCSAPR-9	Capped sq. antiprism (Gyroelongated square pyramid J10)	C_{4v}
	8	CSAPR-9	Capped square antiprism	C_{4v}
	9	JTCTPR-9	Tricapped trigonal prism (J51)	D_{3h}
	10	TCTPR-9	Tricapped trigonal prism	D_{3h}
	11	JTDIC-9	Tridiminished icosahedron (J63)	C_{3v}
	12	HH-9	Hula-hoop	C_{2v}
	13	MFF-9	Muffin	C_s
8	1	OP-8	Octagon	D_{8h}
	2	HPY-8	Heptagonal pyramid	C_{7v}
	3	HBPY-8	Hexagonal bipyramid	D_{6h}
	4	CU-8	Cube	O_h
	5	SAPR-8	Square antiprism	D_{4d}
	6	TDD-8	Triangular dodecahedron	D_{2d}
	7	JGBF-8	Johnson - Gyrobifastigium (J26)	D_{2d}
	8	JETBPY-8	Johnson - Elongated triangular bipyramid (J14)	D_{3h}
	9	JBTP-8	Johnson - Biaugmented trigonal prism (J50)	C_{2v}
	10	BTPR-8	Biaugmented trigonal prism	C_{2v}
	11	JSD-8	Snub disphenoid (J84)	D_{2d}
	12	TT-8	Triakis tetrahedron	T_d
	13	ETBPY-8	Elongated trigonal bipyramid (see 8)	D_{3h}

[1] (a) M. Pinsky, D. Avnir, *Inorg. Chem.*, 1998, **37**, 5575-5582. (b) D. Casanova, J. Cirera, M. Llunell, P. Alemany, D. Avnir, S. Alvarez, *J. Am. Chem. Soc.*, 2004, **126,** 1755-1763. (c) J. Cirera, E.Ruiz, S. Alvarez, *Chem. Eur. J.*, 2006, **12**, 3162-3167. (d) D. Casanova, M. Llunell, P. Alemany, S. Alvarez. *Chem. Eur. J.*, 2005, **11**, 1479-1494. (e) A. Ruiz-Martínez, D. Casanova, S. Alvarez, *Chem. Eur. J.*, 2008, **14**, 1291-1303.

Complex 1 Nine coordinate Dy^{III} center.

	EP -9	OPY -9	HBPY -9	JTC -9	JCCU -9	CCU -9	JCSAPR -9	CSAPR -9	JTCTPR -9	**TCTPR** **-9**	JTDIC -9	HH -9	MFF -9
Dy-1	33.953	23.573	18.854	13.645	9.596	8.589	2.726	1.969	2.303	**1.748**	11.381	11.733	1.971

Complex 2 Eight coordinate Dy^{III} center.

	OP -8	HPY -8	HBPY -8	CU -8	SAPR -8	**TDD** **-8**	JGBF -8	JETBPY -8	JBTPR -8	BTPR -8	JSD -8	TT -8	ETBPY -8
Dy-1	33.518	22.823	12.486	6.610	2.424	**0.990**	14.842	27.021	4.170	3.310	4.982	7.041	22.593

Complex 3 Eight coordinate Dy^{III} center.

	OP -8	HPY -8	HBPY -8	CU -8	SAPR -8	**TDD** **-8**	JGBF -8	JETBPY -8	JBTPR -8	BTPR -8	JSD -8	TT -8	ETBPY -8
Dy-1	33.176	22.930	15.813	12.443	3.068	**1.257**	12.855	27.041	2.204	1.951	3.313	13.060	23.464

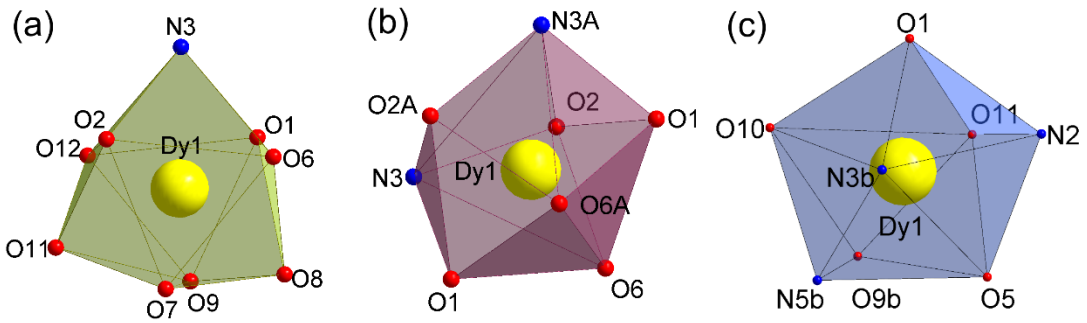

Fig. S1 The coordination geometry of Dy1 in complexes (a) **1**, (b) **2** and (c) **3**.

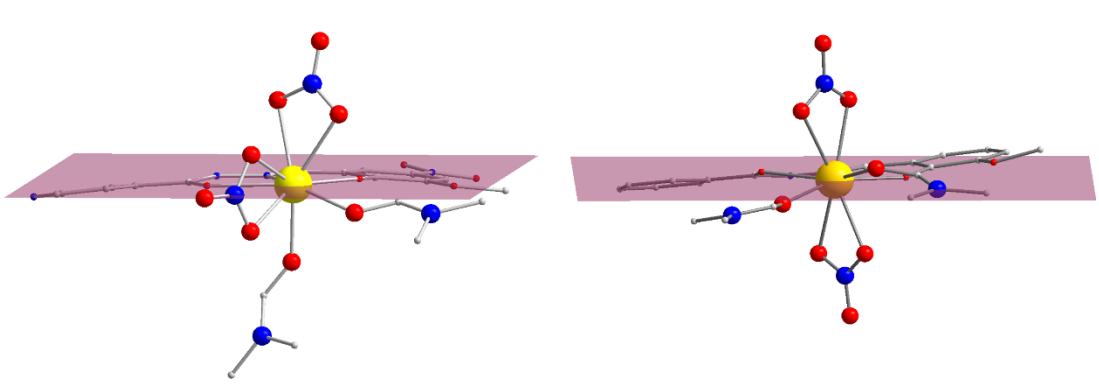

Fig. S2 The coordination environments of complex **1** (Left) and [Dy(hmb)$(NO_3)_2(DMF)_2$] (Right). Color code: Yellow (Dy), Red (O), Blue (N), Gray (C).

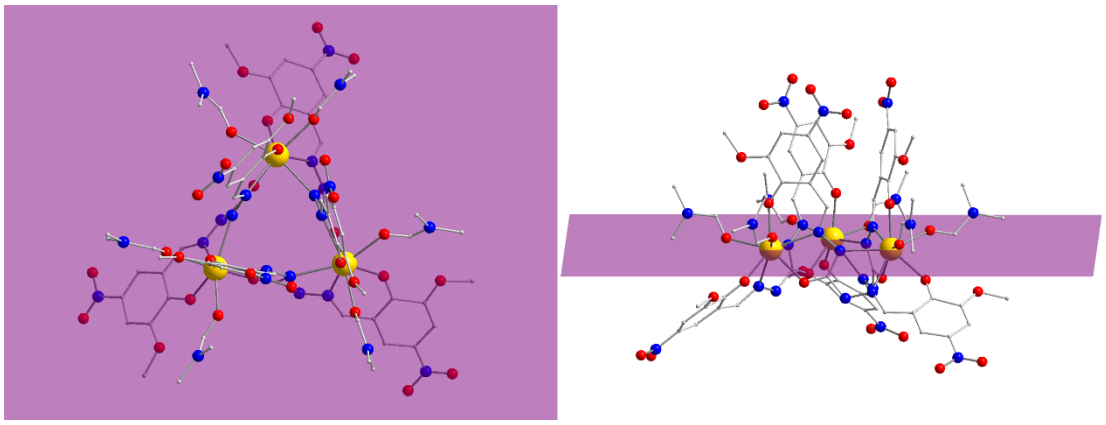

Fig. S3 The Dy_3 triangle plane of complex **3**. Color code: Yellow (Dy), Red (O), Blue (N), Gray (C).

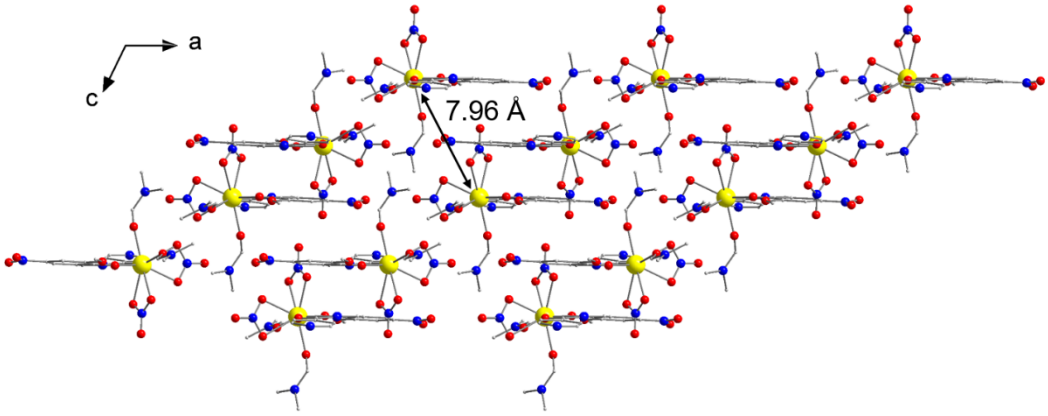

Fig. S4 Packing arrangement along the *b* axis for complex **1**. Color code: Yellow (Dy), Red (O), Blue (N), Gray (C).

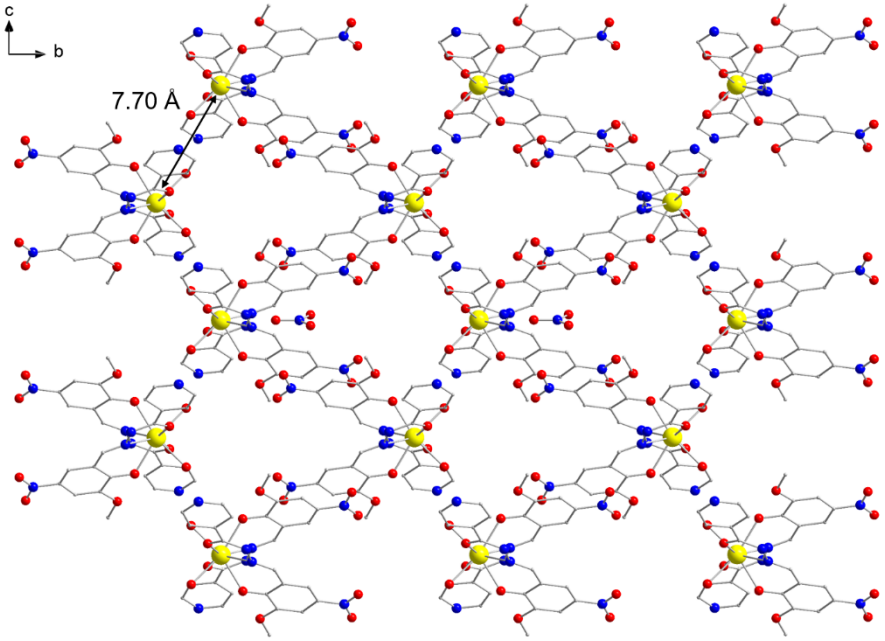

Fig. S5 Packing arrangement along the *a* axis for complex **2**. Color code: Yellow (Dy), Red (O), Blue (N), Gray (C).

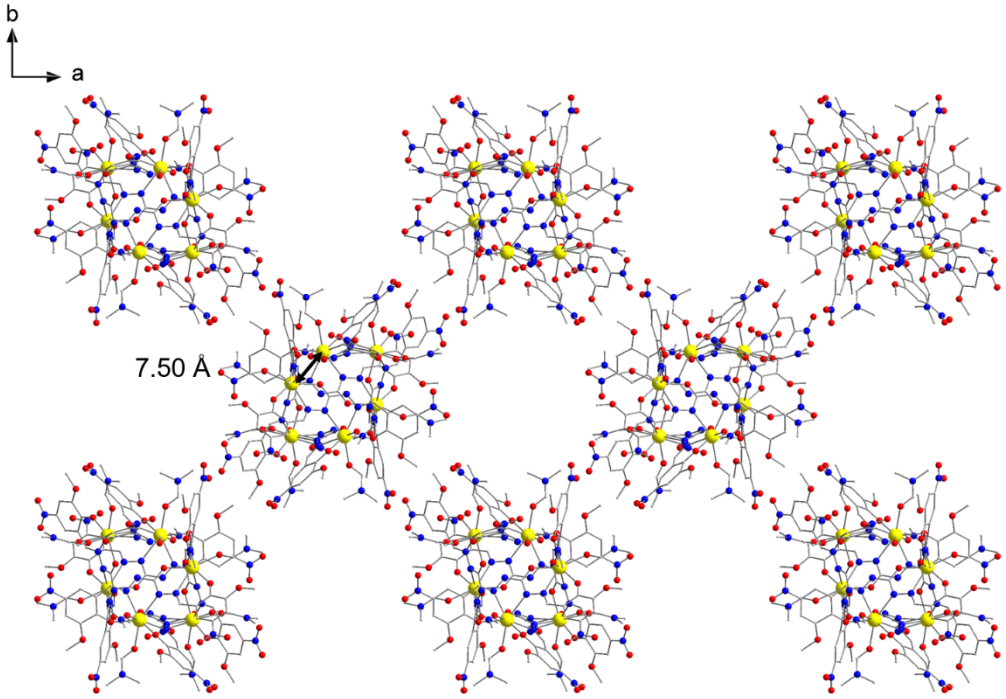

Fig. S6 Packing arrangement along the *c* axis for complex **3**. Color code: Yellow (Dy), Red (O), Blue (N), Gray (C).

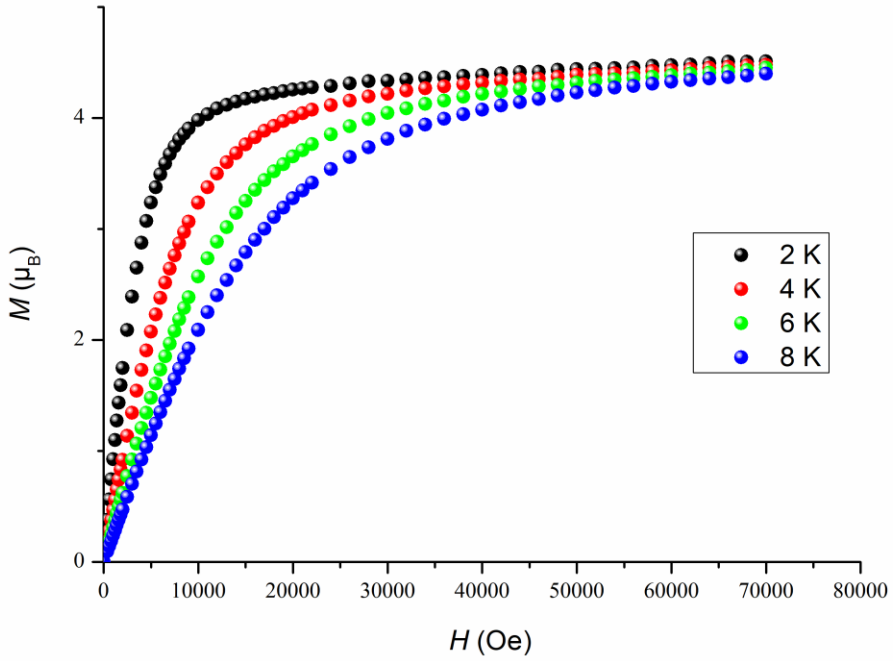

Fig. S7 Field dependence magnetization data at 2 K, 4 K, 6 K and 8 K for complex **1**.

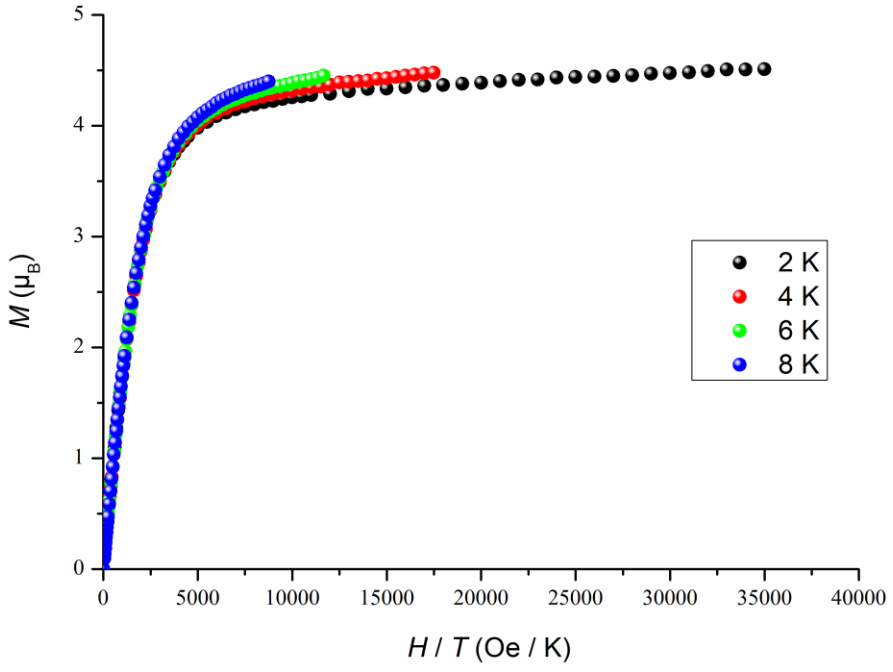

Fig. S8 M vs. H/T plots measured at 2 K, 4 K, 6 K and 8 K for complex **1**.

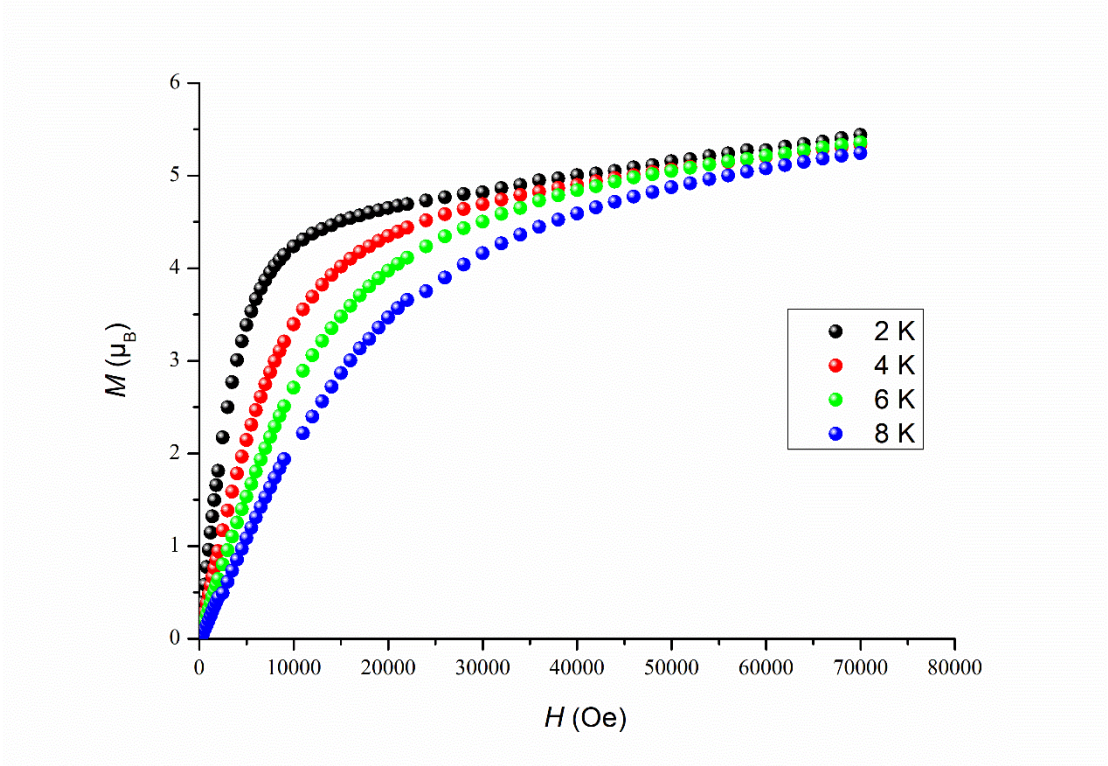

Fig. S9 Field dependence magnetization data at 2 K, 4 K, 6 K and 8 K for complex **2**.

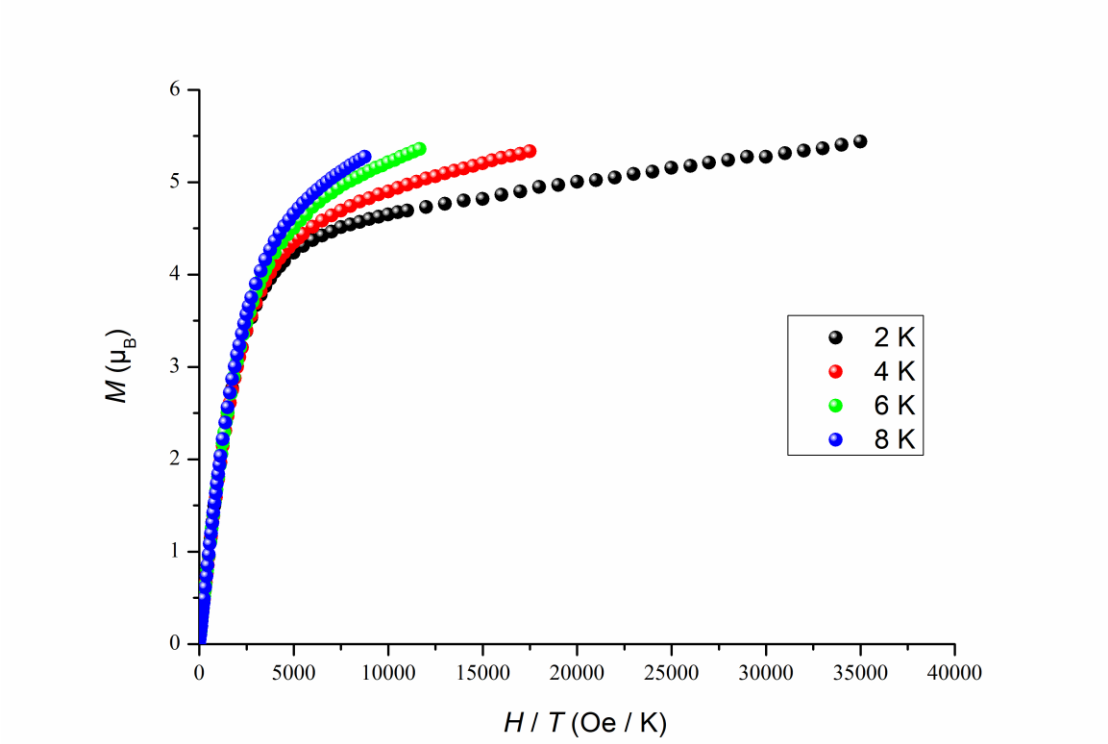

Fig. S10 M vs. H/T plots measured at 2 K, 4 K, 6 K and 8 K for complex **2**.

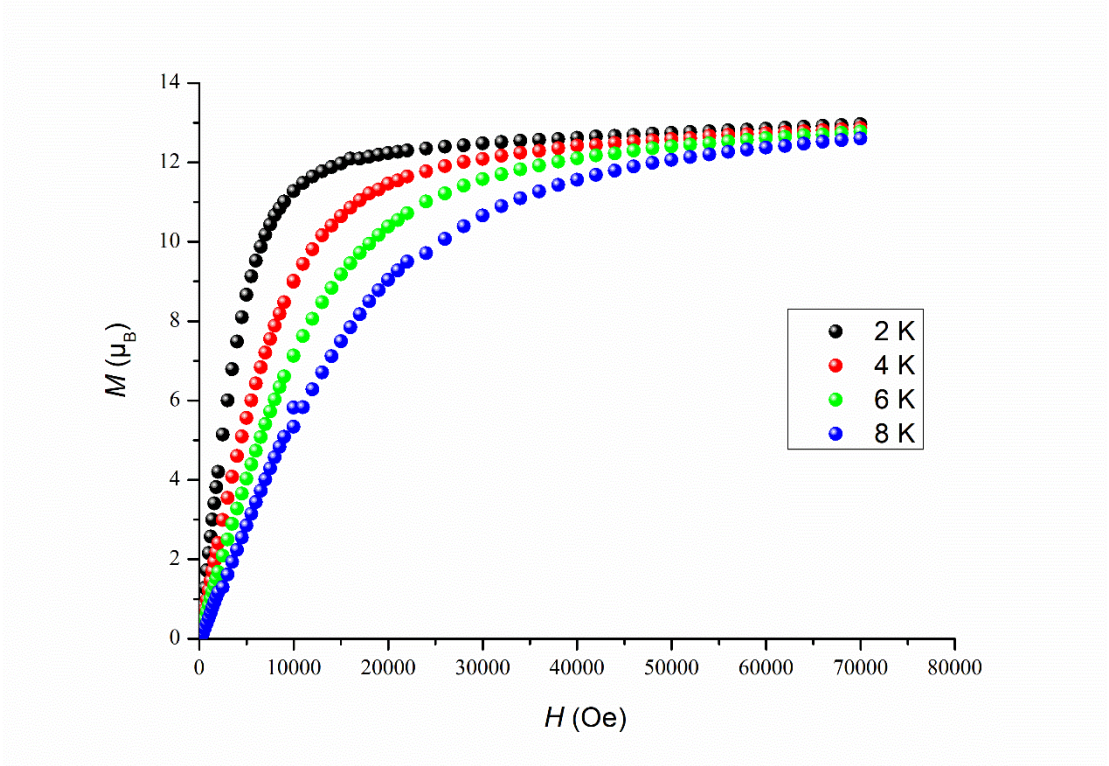

Fig. S11 Field dependence magnetization data at 2 K, 4 K, 6 K and 8 K for complex **3**.

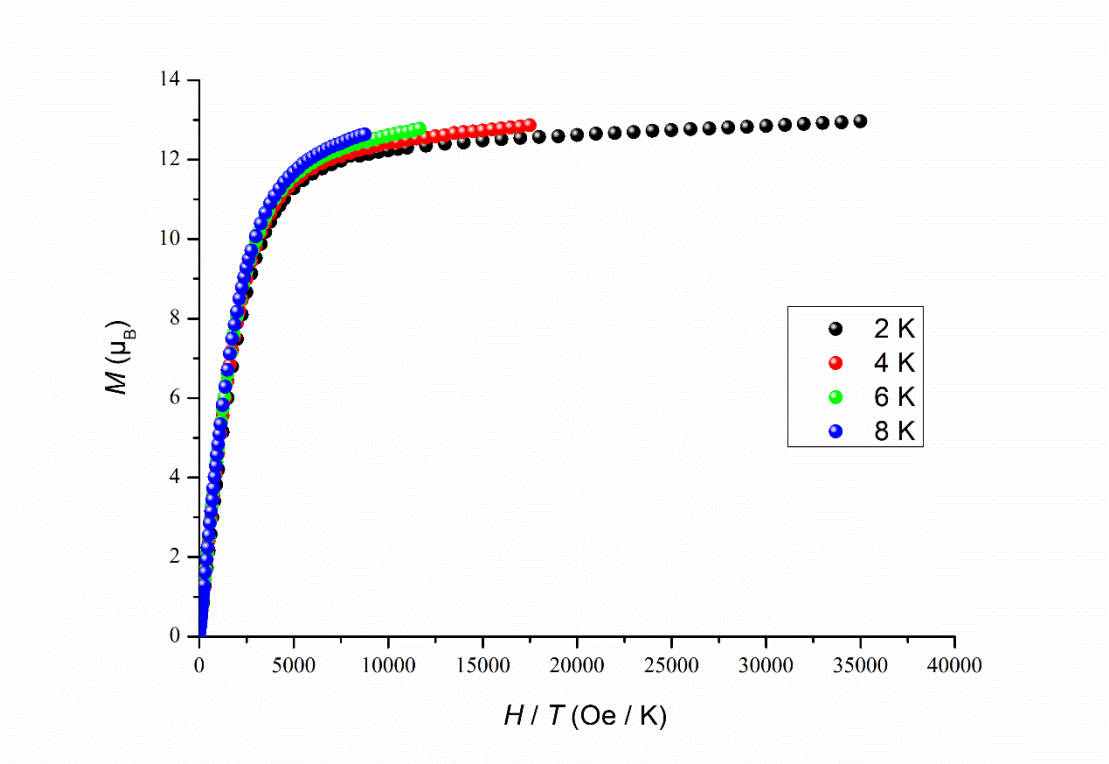

Fig. S12 M vs. H/T plots measured at 2 K, 4 K, 6 K and 8 K for complex **3**.

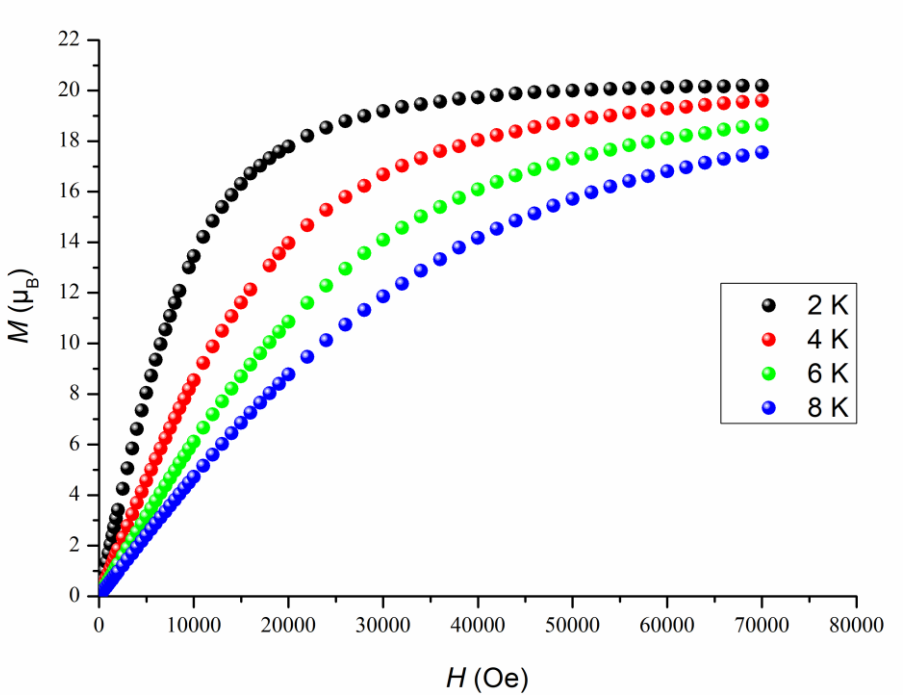

Fig. S13 Field dependence magnetization data at 2 K, 4 K, 6 K and 8 K for complex **4**.

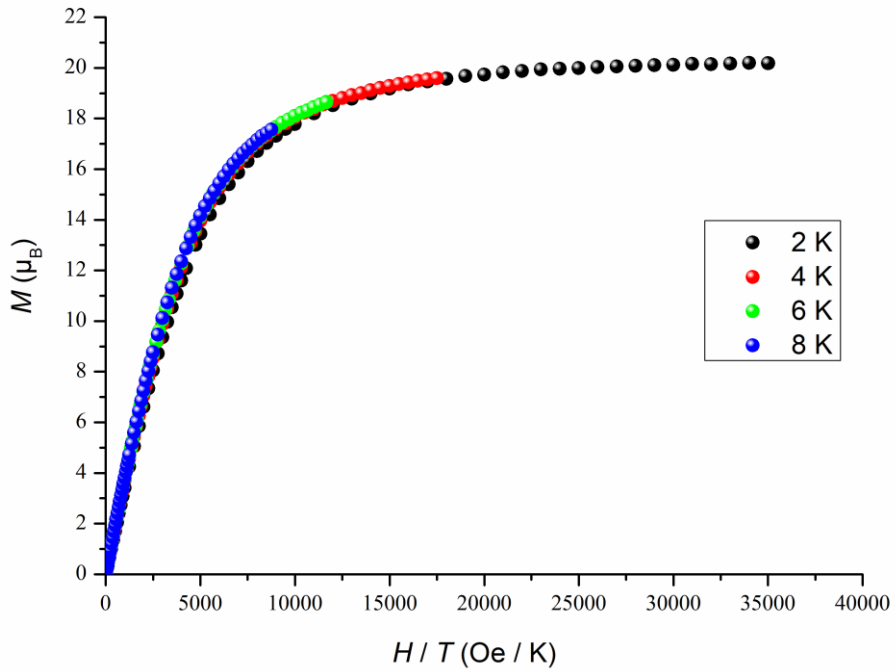

Fig. S14 M vs. H/T plots measured at 2 K, 4 K, 6 K and 8 K for complex **4**.

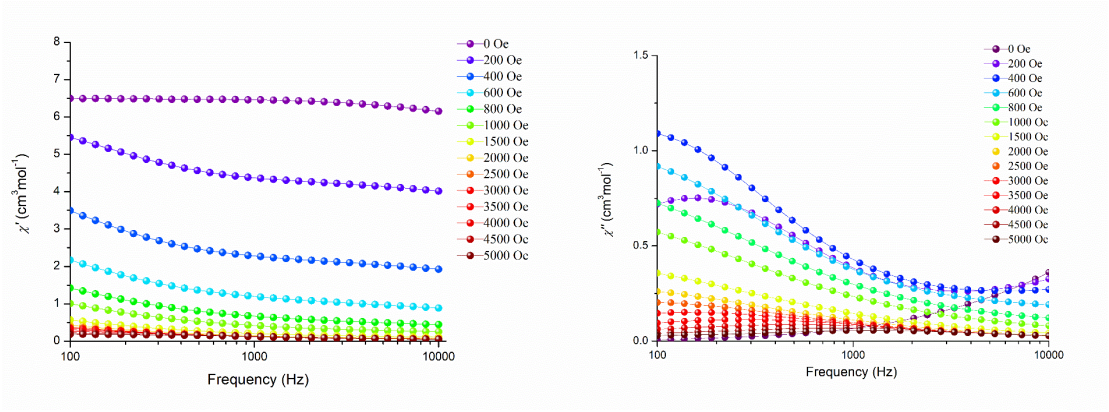

Fig. S15 Field-dependence of the in-of-phase (χ') and out-of-phase (χ") at 1.8 K for complex **1**.

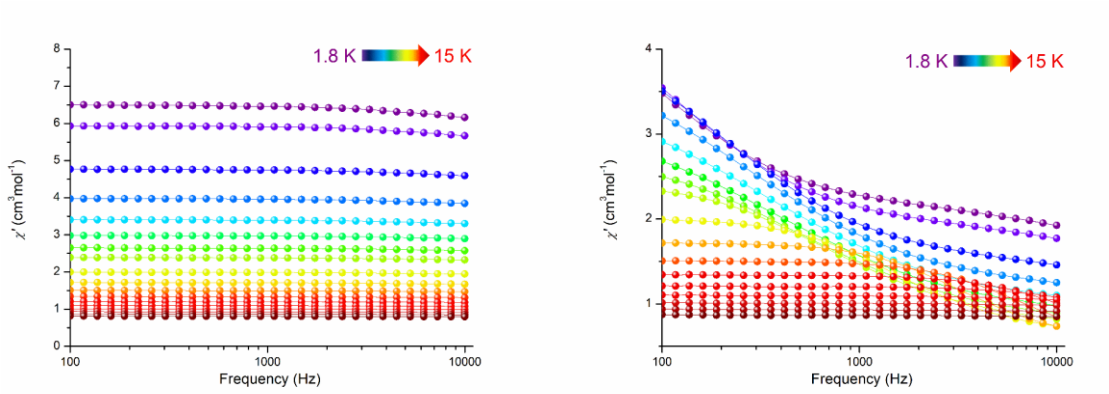

Fig. S16 Frequency dependence of the in-of-phase susceptibility under zero (Left) and 400 Oe (Right) dc field for complex **1**.

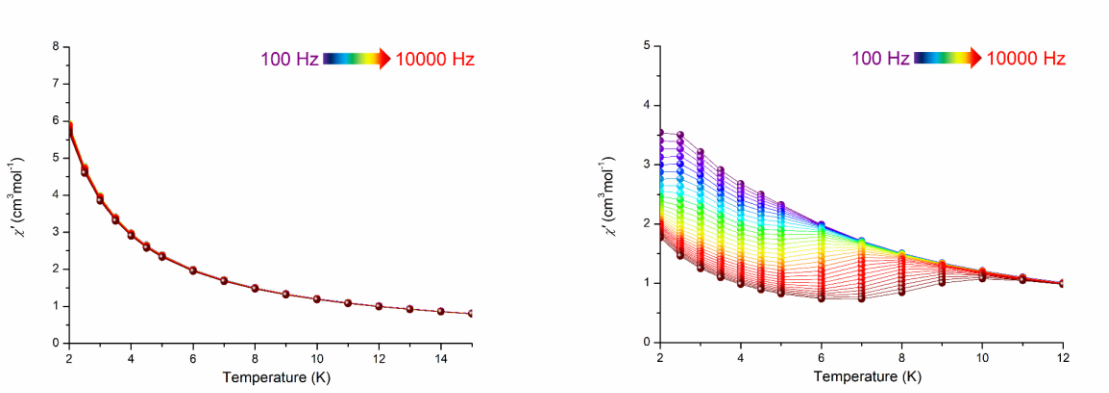

Fig. S17 Temperature dependence of the in-of-phase susceptibility under zero (Left) and 400 Oe (Right) dc field for complex **1**.

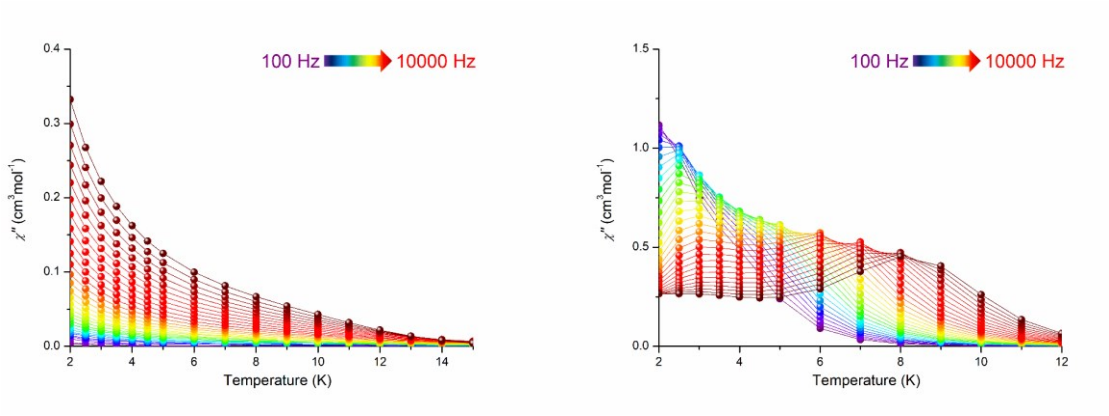

Fig. S18 Temperature dependence of the out-of-phase susceptibility under zero (Left) and 400 Oe (Right) dc field for complex **1**.

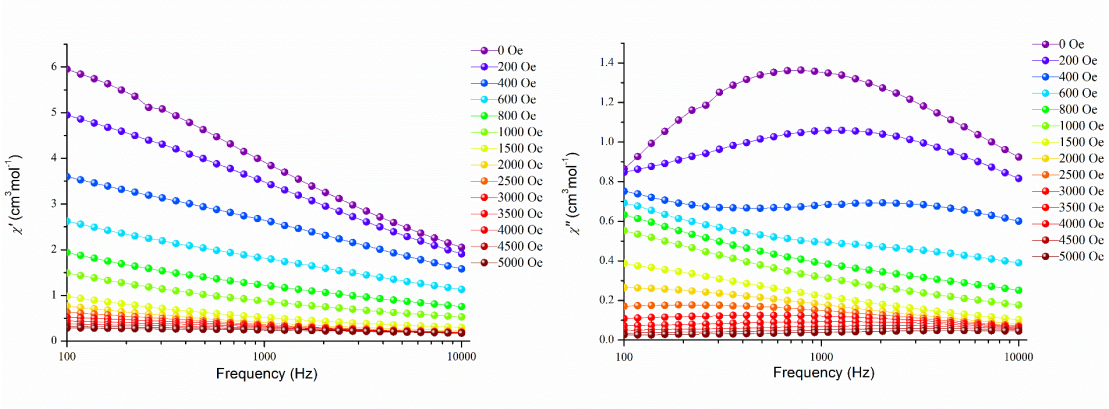

Fig. S19 Field-dependence of the in-of-phase (χ′) and out-of-phase (χ″) at 1.8 K for complex **2**.

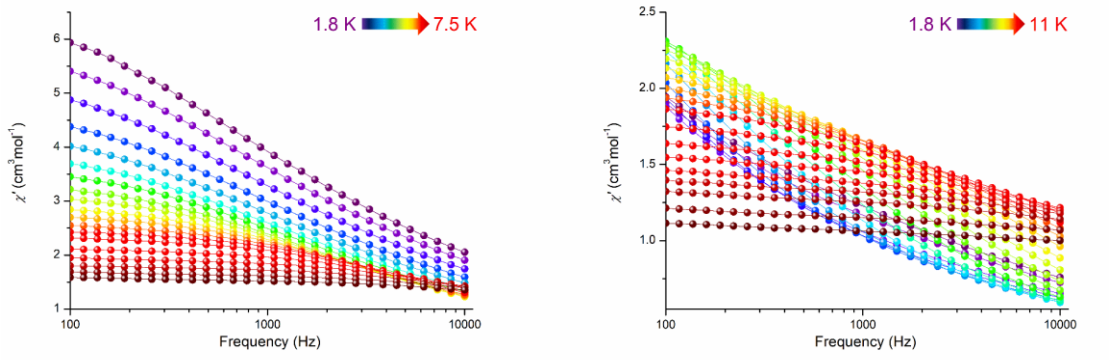

Fig. S20 Frequency dependence of the in-of-phase susceptibility under zero (Left) and 400 Oe (Right) dc field for complex **2**.

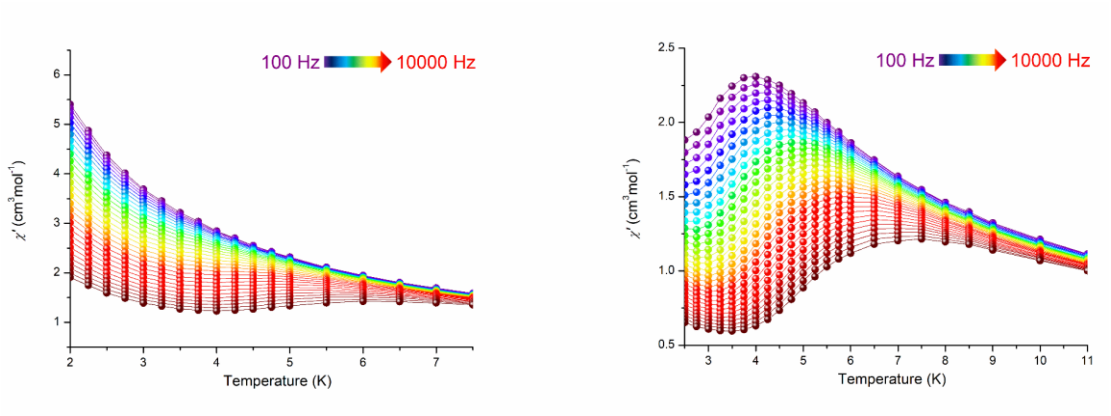

Fig. S21 Temperature dependence of the in-of-phase susceptibility under zero (Left) and 400 Oe (Right) dc field for complex **2**.

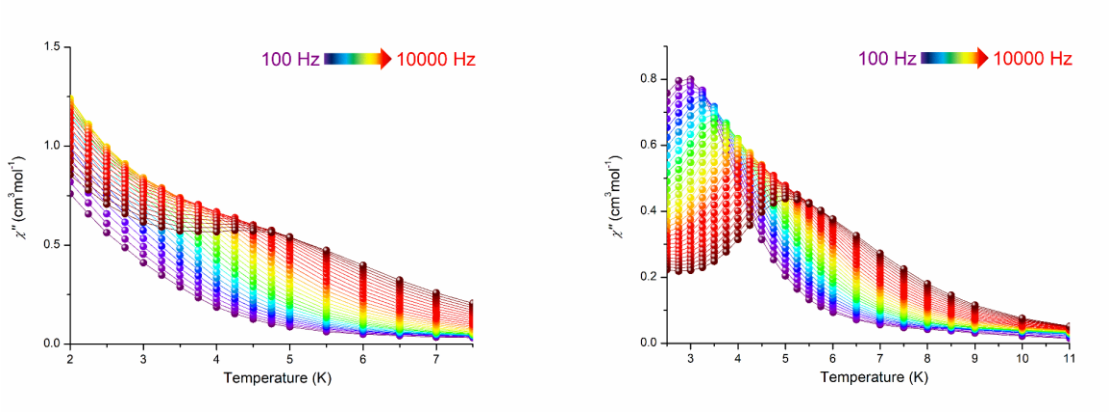

Fig. S22 Temperature dependence of the out-of-phase susceptibility under zero (Left) and 400 Oe (Right) dc field for complex **2**.

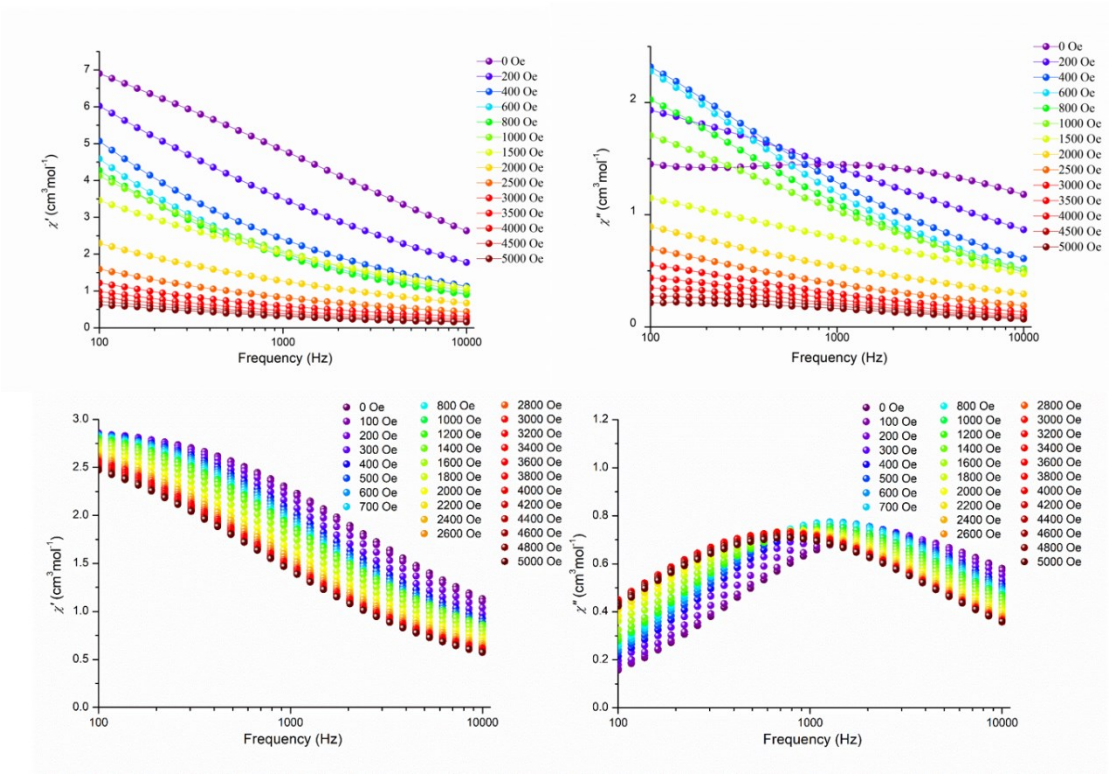

Fig. S23 Field-dependence of the in-of-phase (χ′) and out-of-phase (χ″) at 1.8 K (top) and 10 K (bottom) for complex **3**.

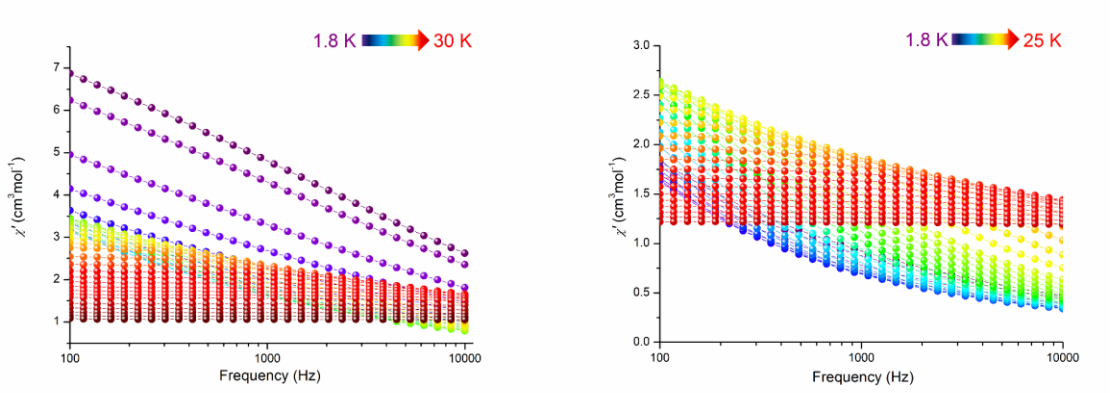

Fig. S24 Frequency dependence of the in-of-phase susceptibility under zero (Left) and 2600 Oe (Right) dc field for complex **3**.

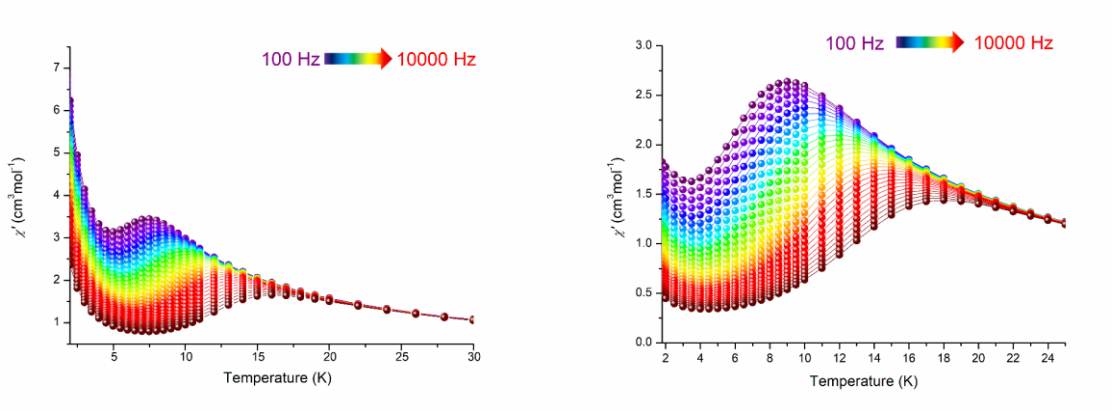

Fig. S25 Temperature dependence of the in-of-phase susceptibility under zero (Left) and 2600 Oe (Right) dc field for complex **3**.

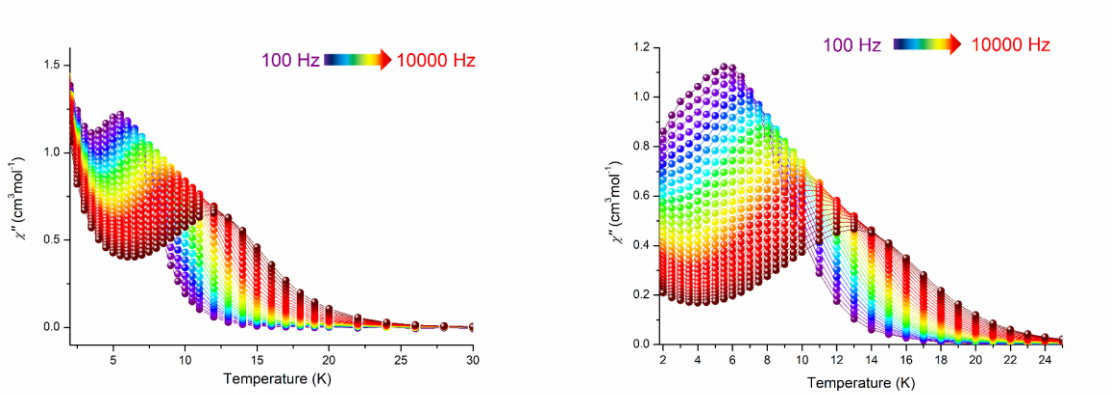

Fig. S26 Temperature dependence of the out-of-phase susceptibility under zero (Left) and 2600 Oe (Right) dc field for complex **3**.

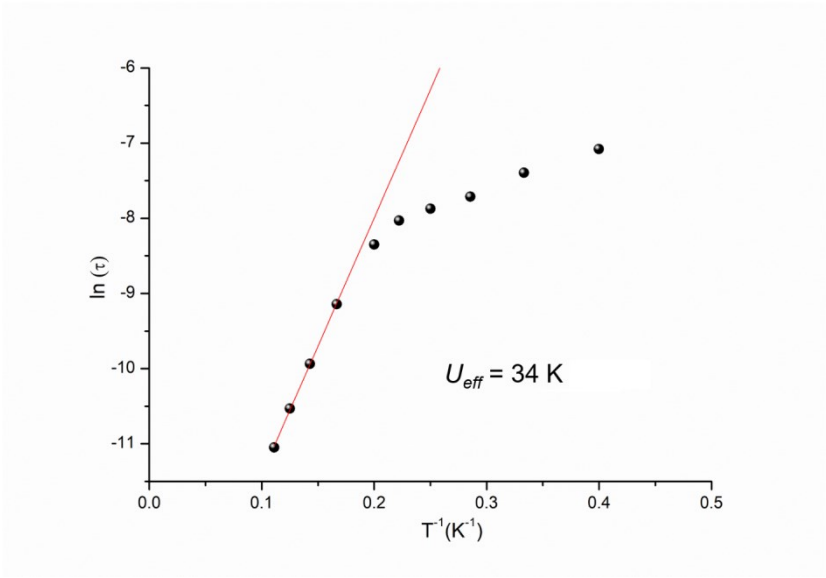

Fig. S27 Arrhenius plots for complex **1** under a 400 Oe dc field. The τ values of anisotropic energy barriers were converted from the frequency, we applied with the maxima χ'' value in each temperature in ac susceptibility measurement. (Fig. 5b)

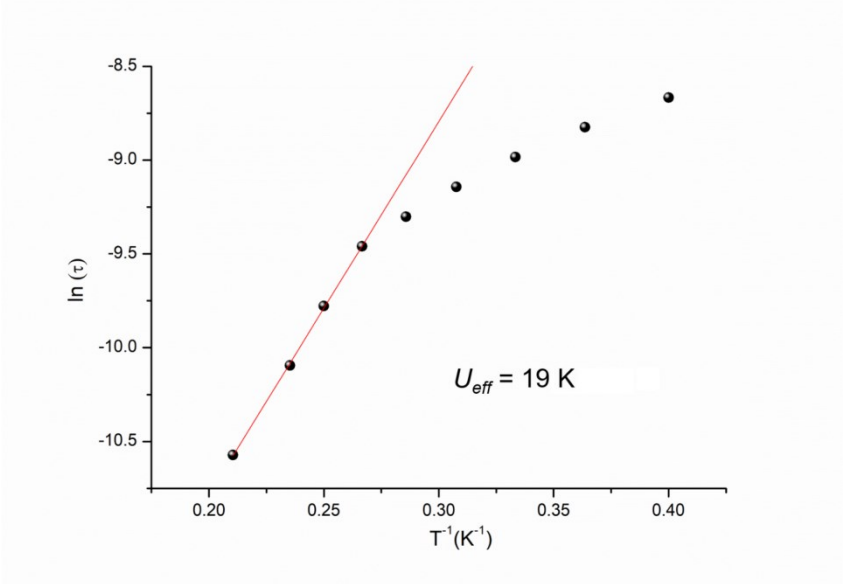

Fig. S28 Arrhenius plots for complex **2** under zero dc field. The τ values of anisotropic energy barriers were converted from the frequency we applied with the maxima χ'' value in each temperature in ac susceptibility measurement. (Fig. 5c)

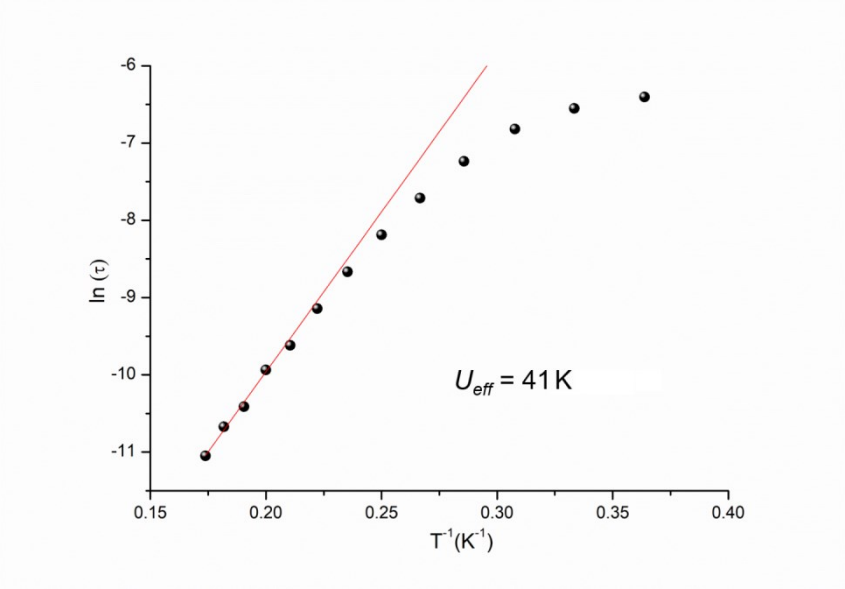

Fig. S29 Arrhenius plots for complex **2** under a 400 Oe dc field. The τ values of anisotropic energy barriers were converted from the frequency, we applied with the maxima χ'' value in each temperature in ac susceptibility measurement. (Fig. 5d)

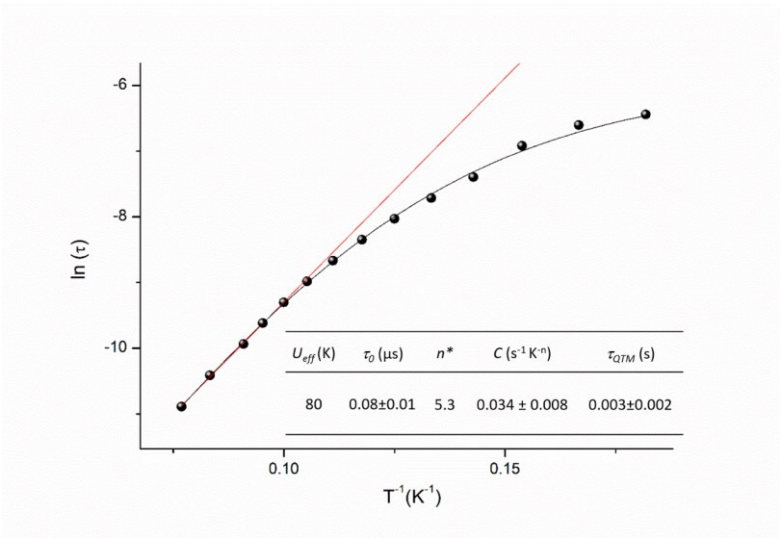

Fig. S30 Arrhenius plots for complex **3** under zero dc field. The τ values of anisotropic energy barriers were converted from the frequency, we applied with the maxima χ'' value in each temperature in ac susceptibility measurement. (Fig. 6a)

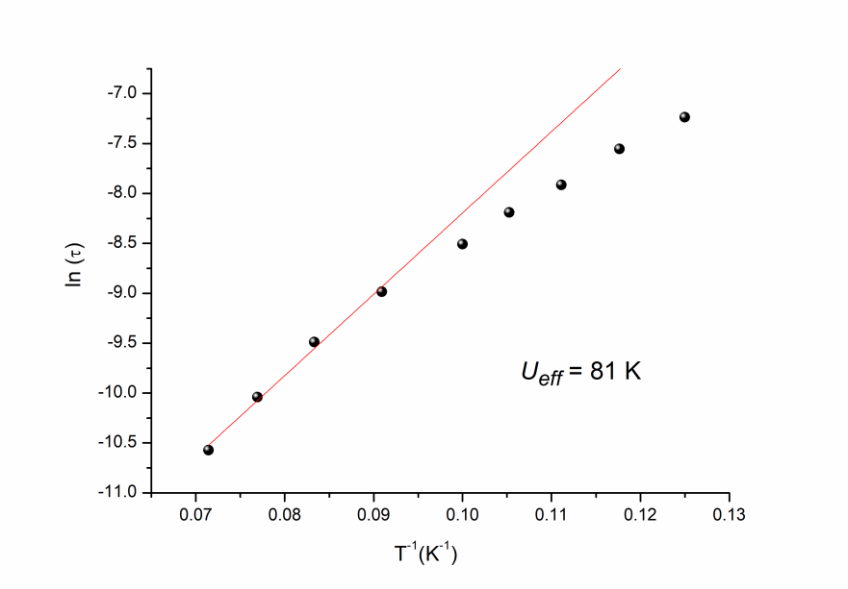

Fig. S31 Arrhenius plots for complex **3** under a 2600 Oe dc field. The τ values of anisotropic energy barriers were converted from the frequency, we applied with the maxima χ'' value in each temperature in ac susceptibility measurement. (Fig. 6b)

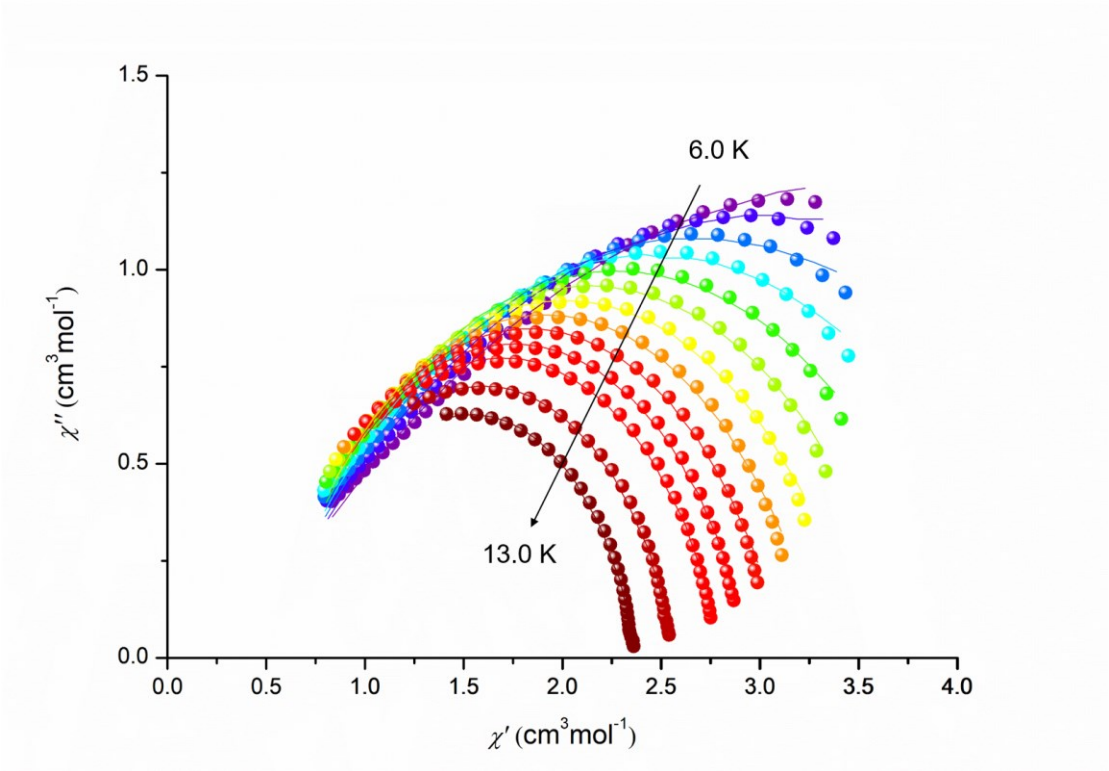

Fig. S32 Cole-cole plots of complex **3** under a zero dc field (CC-Fit.[1]).

[1] Y.-N. Guo, G.-F. Xu, Y. Guoa and J. Tang, *Dalton Trans.*, 2011, **40**, 9953-9963.

Temperature (K)	ChiS	ChiT	Tau	Alpha	Residual
6.0	3.69E-01	6.88E+00	2.55E-03	5.42E-01	2.09E-02
6.5	4.24E-01	5.67E+00	1.14E-03	4.79E-01	2.52E-02
7.0	4.54E-01	4.94E+00	6.42E-04	4.28E-01	2.80E-02
7.5	4.71E-01	4.44E+00	4.11E-04	3.87E-01	2.96E-02
8.0	4.82E-01	4.07E+00	2.81E-04	3.54E-01	3.04E-02
8.5	4.90E-01	3.78E+00	2.01E-04	3.27E-01	2.83E-02
9.0	5.01E-01	3.52E+00	1.47E-04	3.03E-01	2.76E-02
9.5	5.13E-01	3.32E+00	1.10E-04	2.83E-01	2.49E-02
10.0	5.31E-01	3.13E+00	8.37E-05	2.64E-01	2.21E-02
10.5	5.45E-01	2.97E+00	6.40E-05	2.50E-01	1.81E-02
11.0	5.70E-01	2.82E+00	4.98E-05	2.33E-01	1.50E-02
12.0	6.28E-01	2.58E+00	3.16E-05	2.06E-01	9.59E-03
13.0	7.13E-01	2.37E+00	2.14E-05	1.77E-01	5.60E-03

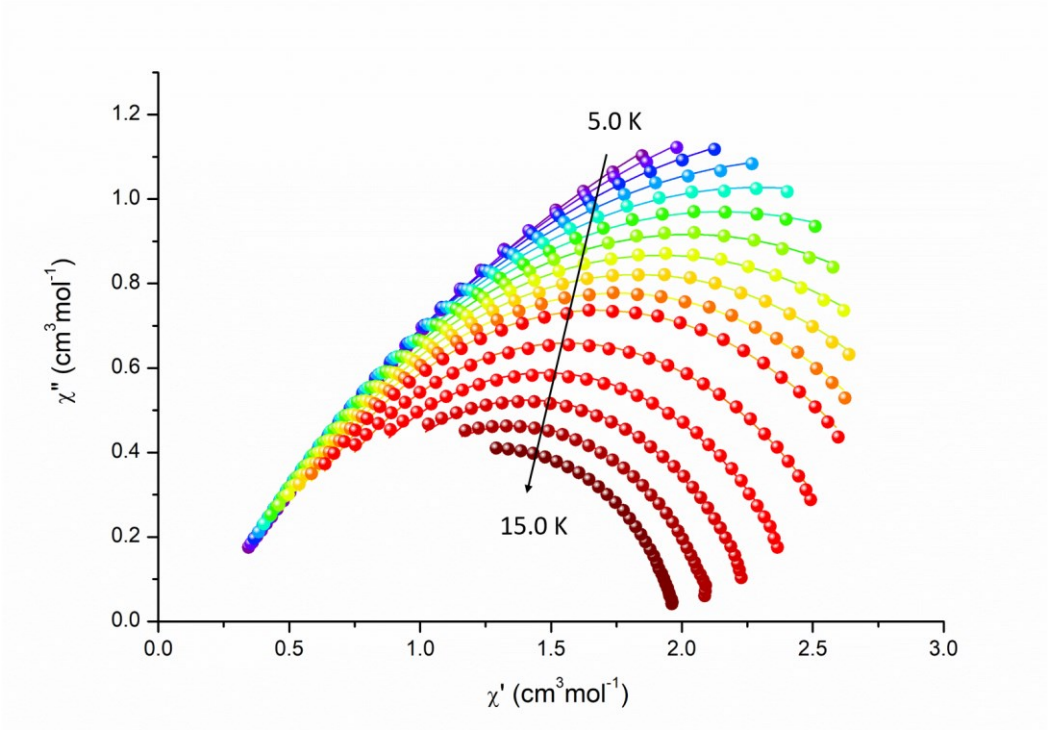

Fig. S33 Cole-cole plots of complex **3** under a 2600 Oe dc field (CC-Fit.[1]).

Temperature (K)	ChiS	ChiT	Tau	Alpha	Residual
5.0	1.88E-01	6.54E+00	8.68E-03	4.76E-01	1.67E-03
5.5	1.96E-01	5.77E+00	5.10E-03	4.57E-01	1.55E-03
6.0	2.02E-01	5.21E+00	3.22E-03	4.41E-01	1.45E-03
6.5	2.09E-01	4.75E+00	2.09E-03	4.28E-01	1.62E-03
7.0	2.19E-01	4.38E+00	1.41E-03	4.15E-01	2.27E-03
7.5	2.29E-01	4.08E+00	9.83E-04	4.05E-01	2.65E-03
8.0	2.42E-01	3.81E+00	6.98E-04	3.96E-01	2.73E-03
8.5	2.58E-01	3.58E+00	5.05E-04	3.88E-01	2.93E-03
9.0	2.76E-01	3.39E+00	3.74E-04	3.81E-01	3.28E-03
9.5	2.96E-01	3.21E+00	2.79E-04	3.75E-01	3.62E-03
10.0	3.20E-01	3.04E+00	2.11E-04	3.68E-01	4.40E-03
11.0	3.70E-01	2.76E+00	1.22E-04	3.57E-01	5.10E-03
12.0	4.29E-01	2.52E+00	7.28E-05	3.46E-01	5.96E-03
13.0	5.05E-01	2.32E+00	4.50E-05	3.32E-01	5.01E-03
14.0	5.91E-01	2.14E+00	2.88E-05	3.15E-01	3.39E-03
15.0	6.78E-01	1.99E+00	1.91E-05	2.98E-01	1.31E-03

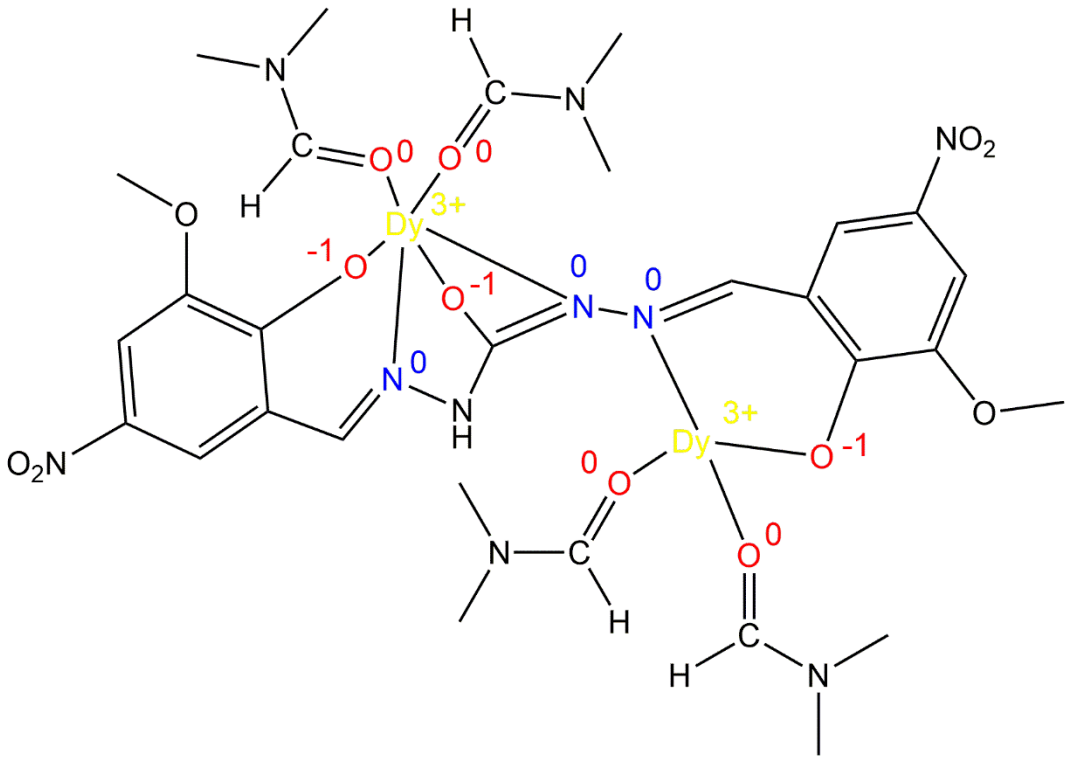

Fig. S34 Partial charges assigned to the formally charged ligands in complex **3**.